The Role of Elasticity in the Anomalous Swelling of Polymer Thin Films in Density Fluctuating Supercritical Fluids

Tadanori Koga,*,[†] Y.-S. Seo,[†] K. Shin,[‡] Y. Zhang,[†] M. H. Rafailovich,*,[†] J. C. Sokolov,[†] B. Chu,[†,§] and S. K. Satija[#]

Department of Materials Science & Engineering, State University of New York at Stony Brook, Stony Brook, New York 11794-2275; Department of Materials Science and Engineering, K-JIST, Kwang-ju, 500-712 Korea; Department of Chemistry, State University of New York at Stony Brook, Stony Brook, New York 11794-3400; and Center for Neutron Research, National Institute of Standards and Technology, Gaithersburg, Maryland 20899

ABSTRACT: In situ neutron reflectivity was used to investigate the effects of density fluctuations on the solubility of supercritical carbon dioxide (scCO$_2$) in polymer thin films. Deuterated polystyrene, deuterated polybutadiene, and the corresponding random copolymer, deuterated styrene-*random*-butadiene copolymer, as well as deuterated poly(methyl methacrylate) were investigated. Data were obtained as a function of pressure under two isothermal conditions ($T = 36$ and 50 °C). All the polymer films used showed anomalous swelling and CO$_2$ sorption on the density fluctuation ridge in the $P–T$ phase diagram of CO$_2$. We found that the magnitude of the swelling was a function of the elasticity of the films rather than the bulk solubility of CO$_2$. The enhanced miscibility of the rubber/CO$_2$ systems, which are very poor in bulk, was found to be almost identical to that of the silicon rubber/CO$_2$ mixture, which is one of the highly miscible polymeric materials under moderate CO$_2$ conditions.

Introduction

Over the past two decades, supercritical fluids (SCFs) have been tremendously utilized as a regeneration solvent in a wide range of technical and chemical processes.[1] The unique features of SCFs are that the solvent quality of SCFs is pressure or/and temperature dependent, while the diffusion coefficient is closer to that of a gas. By varying the external parameters of temperature and pressure, one can control the interactions between the polymer and the fluid environment. In particular, much attention has been focused on supercritical carbon dioxide, scCO$_2$, since CO$_2$ has a moderate critical point with $T_c = 31.3$ °C and $P_c = 7.38$ MPa and is an environmentally clean solvent.

The other special characteristic of SCFs is large density fluctuations in these systems. According to the molecular dynamics simulation of a two-dimensional Lennard-Jones fluid, such fluctuations in pure solvent cause inhomogeneous regions of high and low density, which is represented by the correlation length, ξ.[2] As the critical point of a fluid is approached, ξ and the isothermal compressibility, κ_T, diverge.[3] Density fluctuations, $\langle (\Delta N)^2 \rangle / \langle N \rangle$, are expressed by using κ_T

$$\langle (\Delta N)^2 \rangle / \langle N \rangle = (N/V) \kappa_T k_B T \qquad (1)$$

where k_B is the Boltzmann constant and T is the thermodynamic temperature.[3] If the κ_T values are known as a function of temperature and pressure, we can discuss the thermodynamic behavior in $\langle (\Delta N)^2 \rangle / \langle N \rangle$ of SCFs. Figure 1a shows the $\langle (\Delta N)^2 \rangle / \langle N \rangle$ values of CO$_2$ under the isobaric conditions near the critical point. To
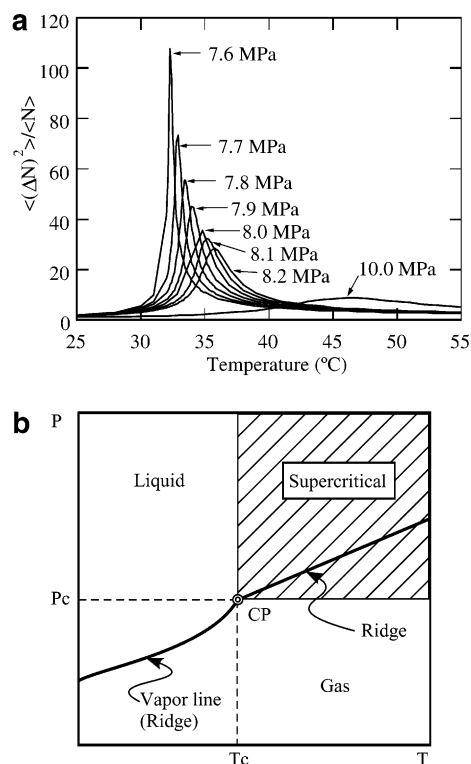

Figure 1. (a) Calculated density fluctuations using the equation of state of CO$_2$. (b) Schematic phase diagram of CO$_2$ near the critical point. Critical point is denoted as CP. Solid line represents the ridge of CO$_2$ reported in ref 5.

obtain the κ_T values of CO$_2$, we used the equation of state given by Huang et al.[4] These calculated $\langle (\Delta N)^2 \rangle / \langle N \rangle$ values are in good agreement with those previously reported from small-angle X-ray scattering measurements.[5] From the figure we can see that the characteristic features of density fluctuations in the supercritical region are (i) there is a peak in each lateral curve, (ii) the amplitude of the fluctuation diverges as the critical

[†] Department of Materials Science & Engineering, SUNY.
[‡] K-JIST.
[§] Department of Chemistry, SUNY.
[#] National Institute of Standards and Technology.
* Corresponding authors: e-mail tkoga@notes.cc.sunysb.edu; mrafailovich@notes.cc.sunysb.edu.

point is approached, and (iii) the width of the peak broadens with increasing pressure. As shown in Figure 1b, the locus of the peaks in $\langle (\Delta N)^2 \rangle / \langle N \rangle$ curves forms the ridge of density fluctuations. The ridge is continuous across T_c and separates the more liquidlike and more gaslike regions in the supercritical region.[5,6] In the region below the critical point, the ridge corresponds to the vapor line. In the supercritical region, there is a memory of the vapor line; that is the ridge. This ridge is not specific to CO_2 and is a general feature for the substances, such as H_2O, CF_3H, Ar, and Hg.[6]

Thermodynamic properties of $scCO_2$–polymer phase systems, such as swollen volume, solubility, and viscosity, are very important in various polymer processing operations. Several groups reported the effects of temperature and pressure of CO_2 on the swelling of bulk polymers, such as polystyrene (PS),[7–9] poly(methyl methacrylate) (PMMA)[7–10] and polycarbonates (PC),[7,10] silicone rubber (SR),[11–13] and poly(dimethylsiloxane) (PDMS),[14,15] in a range of sub- and/or supercritical regions. The typical features of bulk swelling and solubility data show an "S"-shaped isotherm with an inflection point in the vicinity of P_c. The thermodynamics of the bulk polymer–supercritical mixtures have been successfully described by the lattice models, such as the Sanchez–Lacombe (S–L) equation of state or the Panayiotou–Vera equation of state, which holes or vacancies have been introduced to simulate the effect of the change in volume.[7,8,14–16]

On the other hand, very little is known about the interaction of CO_2 with polymer thin films, which are of significant technological importance in coating, lubrication, and adhesion. The behavior of CO_2 with polymer thin films may differ from that in the bulk, since one must also consider the effect of surface interactions and confinements. It is well-known that the presence of an interacting surface can also modify the physical properties of thin films such as viscosity, diffusion coefficient, and possibly glass transition temperature.[17] The introduction of a third component, such as a solvent that can compete with the polymer for adsorption to the surface, introduces yet another variable in determining the properties of thin films. The technical difficulties involved in delivering the probe beams, such as neutron and laser beams, into high pressure vessels have only recently been overcome. By using in situ neutron reflectivity (NR), we clarified that the large density fluctuations of CO_2 enhanced the swelling of polymer thin films at the density fluctuation ridge even when the bulk miscibility of the polymer with CO_2 was very poor.[18] Because of its large penetration depth, NR is an ideal technique to determine the in situ thickness, composition, and interfacial structure of polymer thin films immersed in fluids or gases, under high pressure in thick walled vessels. The functional form of the dilation amplitude followed that of the calculated density fluctuations as a function of temperature and pressure. Sirard et al. reported the swelling behavior of PDMS and PMMA thin films in contact with CO_2 using ellipsometry.[19,20] They reported that the swelling behavior was different from that of the bulk polymers, and the swelling maximum in PMMA was observed at the pressure where the compressibility of CO_2 exhibits a maximum.[20] However, they were only able to study low pressures up to 12 MPa and were not able to determine the concentration profile of the polymers.

Table 1. Material Characteristics of Polymers Used in This Work

polymer	M_w (10^3 g/mol)	M_w/M_n	$\phi_{1,4}$ (%)^a	ϕ_{ps} (%)^b
d-PB1	264	1.15	80	
d-PB2	131	1.06	80	
d-SBR	84	1.08	60	47
d-PMMA	137	1.08		
d-PS	155	1.03		100

^{a} Volume fraction of 1,4-linkage in d-PB. ^{b} Volume fraction of d-PS component.

The polymers studied vary greatly in their miscibility in the presence of CO_2. To explore whether this is a universal phenomena, we compare the swelling characteristics for several classes of polymers, i.e., deuterated PS (d-PS), deuterated polybutadiene (d-PB), and the corresponding random copolymer, deuterated styrene-*random*-butadiene copolymer (d-SBR), as well as deuterated PMMA (d-PMMA) in a wide range of CO_2 pressures up to 70 MPa under two isothermal conditions ($T = 36$ and 50 °C). Comparisons between the glassy and rubbery polymers as well as between random copolymers and homopolymers provided us significant insights into the swelling mechanism of polymer thin films in the presence of density fluctuations of CO_2.

Experimental Section

Materials. One of the unique advantages of neutron measurements is that the scattering intensity from a polymer molecule is quite enhanced by using deuterium labeling of the polymer samples. Rubbery polymers were obtained from Polymer Source, and glassy polymers were obtained from Polymer Laboratories. Their molecular characteristics are listed in Table 1. Silicon wafers for NR experiments (7.5 cm diameter, 8 mm thickness) were first placed into a buffered solution with a mixture of H_2SO_4:H_2O_2 = 1:1 at $T = 100$ °C for 1 h and rinsed with deionized water. They were then etched by HF:H_2O = 3:7 solution to remove the native oxide layer. The polymers were dissolved into toluene, and the homogeneous solutions were filtered through a Millipore film of 0.45 μm pore size. The films were spun-cast onto the clean Si substrates with a rotation speed of 2500 rpm. The film thickness was measured by an ellipsometer (AutoE1-II). The as-cast films were then dried in a vacuum oven for 0.5–5 h at 120–150 °C, which depends on the polymers, to relax strains induced in the spinning process. To avoid sample degradation and memory of the pressure history, we used fresh samples for each isothermal set of experiments.

High-Pressure Cell. Figure 2a shows a schematic view of the high-pressure cell for NR experiments. The body of the high-pressure cell was machined from 4340 steel. Sapphire was selected for the optical window material because of high transparency for neutrons (more than 90%).[21] Furthermore, sapphire has high tensile strength (elastic limit 448 MPa), resistance to corrosion, high-energy damage threshold, and low absorbance. Two cylindrical sapphire windows (2.4 cm in thick, o.d. 5 cm) were installed for transmitting the incident beam and for receiving the reflected beams. The sealing was achieved by a combination of a Teflon and a nylon gasket placed between the sapphire windows. The cell had a volume of about 10 mL and a maximum pressure rating of 140.0 MPa. CO_2 used in this study has a purity of 99.9%. CO_2 was loaded into the cell by means of a hand-operated syringe pump (HIP Equip.) to the desired pressure. Prior to pressurization, the air space is purged with the gas at low pressure. Since only amorphous silicon and fluorinated polymers are "CO_2-soluble" at readily accessible conditions ($T < 100$ °C, $P < 50$ MPa),[22] the successive pressurized and depressurized processes were enabled for NR measurements. Figure 2b shows the general experimental arrangements for NR experiments. CO_2 pressure inside the cell was monitored by using an OMEGADYNE pressure transducer (TH-1) with a pressure gauge meter
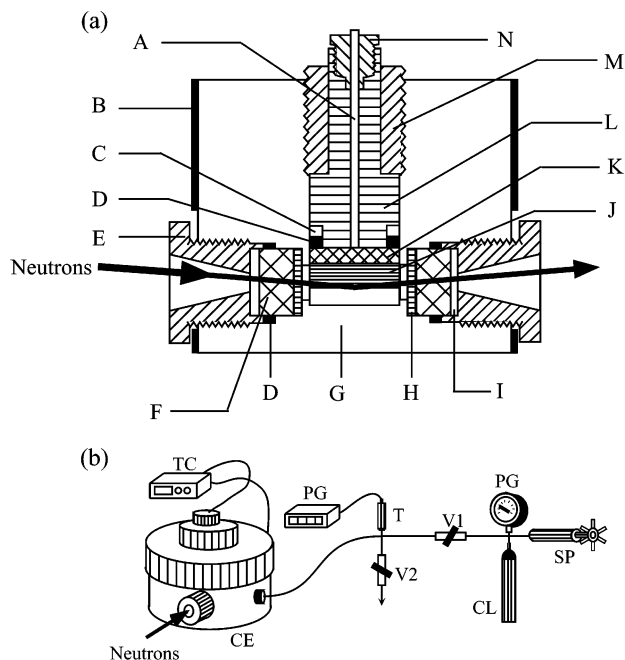
(a)

(b)

Figure 2. Schematic diagram of (a) high-pressure cell and (b) experimental configuration for NR experiments: (A) thermocouple, (B) heater, (C) backup ring, (D) Teflon O-ring, (E) retainer, (F) sapphire windows, (G) chamber, (H) Teflon gasket (I) nylon gasket, (J) Si wafer (K) Al spacer, (L) cover, (M) main nut, (N) HF4 connection, (CL) CO_2 cylinder, (SP) hand-operated syringe pump, (PG) pressure gauge, (V1) inlet valve, (V2) release valve, (T) pressure transducer, (TC) temperature controller, (CE) high-pressure chamber.

(INFS-0001-DC1). The temperature of the cell was controlled by a temperature controller (CAL Controls) equipped with heaters that were installed on the outer side of the cell and a thermocouple (Rama Co.). The temperature of the system was controlled with an accuracy of ±0.1 °C, and the stability of pressure during the measurements was less than ±0.2%.

Neutron Reflectivity. The specular reflectivity measurements were performed at the National Institute of Standards and Technology Center for Neutron Research (NCNR) NG-7 reflectometry. The wavelength of neutrons was 4.7 Å with $\Delta\lambda/\lambda$ = 2%. Because of high absorption of neutrons in compressed CO_2, the incident and reflected beams passed through the Si wafer with a transmission of 0.90 relative to air. Data were obtained both by successively increasing the pressure and then slowly decreasing the pressure under isothermal and isobaric conditions. It should be noted that, as previously described,[23] the swelling maximum at the ridge in the first pressurized processes was different from those for further cycles due to the pinning of the film onto the Si substrate. In addition to this factor, d-PS thin films showed a hysteresis in the swelling isotherms at low pressures between the pressurized and depressurized cycles due to the glass−liquid transition of the polymers.[20,23−27] Accordingly, the swelling measurements were conducted in the pressurization process by using pre-CO_2-annealed samples, which were immersed in an scCO$_2$ condition (T = 36 °C and P = 20.0 MPa) for 1 h and were quickly depressurized to atmospheric pressure at constant temperature. We confirmed that the film qualities, such as thickness and roughness, were identical to those of the unswollen thickness before and after the treatment. The equilibrium swelling of the glassy polymer thin films was achieved by 0.5 h annealing at the desired pressure prior to data collection. The equilibration time for the rubbery polymers in the vicinity of the ridge was much longer (∼5 h), as will be discussed later.

Since the background scattering from pure CO_2 increased dramatically near the critical point,[18] we monitored the background scattering for each pressure condition as well. The NR data corrected for the background scattering were analyzed by comparing the observed reflectivities with the calculated ones based on model density profiles having three free parameters: film thickness, scattering length density (SLD), and interfacial root-mean-square (rms) roughness (σ) between polymer and CO_2 layers, which was approximated by an error function.[28] From the X-ray reflectivity measurements, the thickness of a silicon oxide layer was determined to be 10 Å. The thickness was kept constant in all the fitting procedures. The neutron scattering length density (SLD) of CO_2 solvent, which is variable from 0.004×10^{-6} to 2.75×10^{-6} Å^{-2} in the pressure range of $0.1 < P < 70.0$ MPa at T = 36 and 50 °C, was calculated from the bulk density obtained by the equation of state of CO_2.[4]

Results

(a) d-PS Thin Films. As we already mentioned, the significant advantage of the compressed gases as solvents is that the solvent quality can be easily tuned through temperature and pressure. It is well-known that CO_2, by variation of temperature and pressure, can assume the equivalent solvent properties of a range of conventional solvents from pentane to pyridine. The solubility parameters for compressed gases can be calculated from the empirical equation derived by Gidding et al.[29]

$$\delta_1 = 1.25P_c^{1/2}[\rho_r/\rho_r(\text{liq})] \qquad (2)$$

where P_c is the critical pressure of the supercritical fluid, ρ_r is the reduced density of the fluid, and $\rho_r(\text{liq})$ is assumed to be 2.66, a typical reduced density of the fluid in the liquid state. The calculated δ_1 values by eq 2 range from 0 to approximately 8 (cal/cm^3)$^{1/2}$ with increasing pressure at constant temperatures used for the NR measurements. Although the interaction parameter χ is expressed by two components, i.e., the enthalpic (χ_H) and entropic (χ_s) components of the thermodynamic interactions, in this instance, we consider only χ_H as a measure of the solvent quality because χ_H can be easily calculated by the solubility parameters to obtain a qualitative check. χ_H is given as follows:

$$\chi_H \propto (\delta_1 - \delta_2)^2 \qquad (3)$$

where δ_2 is the solubility parameter of the polymers, which are ∼8.5 (cal/cm^3)$^{1/2}$ for the typical polymers, such as PS, PB, and PMMA.[30] Therefore, the solvent quality of compressed CO_2 gas in a polymer is improved as the pressure is increased at constant temperature. Note that the solubility parameters of the polymers also change as a function of temperature and pressure, but the degree of the change in δ_2 is negligible compared with that of CO_2.

Figure 3a shows representative NR curves of d-PS thin film at T = 36 °C. The reflectivity was plotted as a function of the momentum transfer normal to the surface, $q_z = 4\pi \sin\theta/\lambda$, where θ is the glancing angle of incidence and λ is the neutron wavelength, respectively. The solid lines are fit to the single layer density profiles shown in Figure 3b. As shown in the figure, we find that good fits could be obtained with uniform concentration of CO_2 in the polymer layer, and no preferential adsorption of either CO_2 or polymer occurred at the Si substrate surface. The thickness of the layer, which was initially 445 Å thick, increased to 513 Å at P = 8.2 MPa and then decreased again to 483 Å upon compression up to P = 20.6 MPa. The interfacial root-mean-square (rms) roughness (σ) between the polymer and CO_2 layers, which was initially 10 Å at

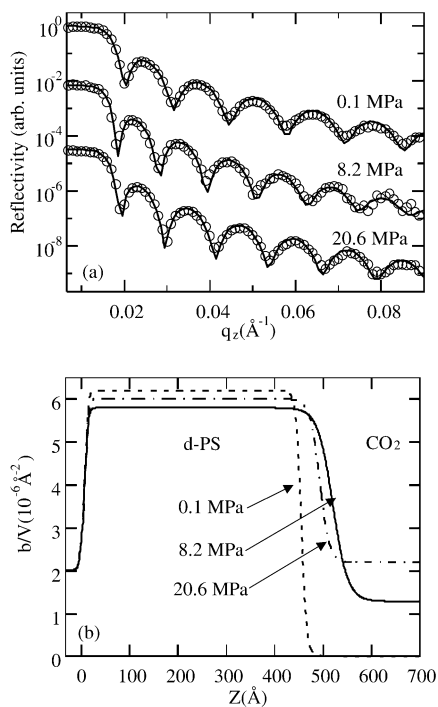**Figure 3.** (a) Representative reflectivity data for d-PS at $T = 36\ °C$. Consecutive reflectivities have been offset from each other for clarity. Solid lines represent the reflectivity calculated from corresponding concentration profiles shown in (b): solid line, $P = 0.1$ MPa; dotted lines, $P = 8.2$ MPa; solid-dotted lines, $P = 20.6$ MPa.
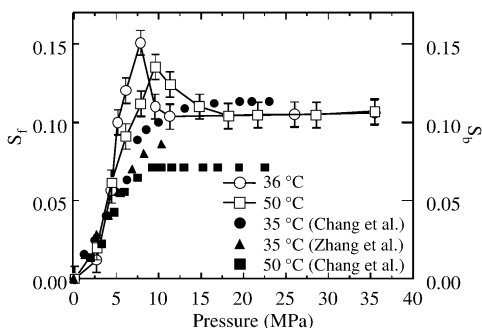

Figure 4. Comparison of swelling isotherms between d-PS thin film and bulk in CO_2. Bulk data are from refs 8 and 9.

atmospheric pressure, increased to 28 Å at $P = 8.2$ MPa and then decreased again to 18 Å at $P = 20.6$ MPa. It should be noted that the roughness after the complete depressurization to atmospheric pressure decreased to about 10 Å, indicating that large voids such as those reported in bulk PS films do not occur.[31,32] This is further confirmed by an atomic force microscopy (AFM) scan of the surface topography from d-PS thin film exposed to several cycles of in beam pressurizing and depressurizing, where the surface appears flat with the same rms roughness of ∼10 Å as that obtained from the NR results.[23]

In Figure 4 we plot the linear dilation (S_f) of the d-PS films at $T = 36$ and $50\ °C$. The linear dilation was calculated from the equation $S_f = (L - L_0)/L_0$, where L and L_0 are the measured thickness of the swollen and unswollen polymer thin films, respectively. The maximal S_f values were 0.15 at $T = 36\ °C$ and $P = 8.2$ MPa and 0.13 at $T = 50\ °C$ and $P = 10$ MPa, which occur along the density fluctuation ridge. Similar swelling behavior was previously reported for a different molecular weight d-PS ($M_w = 957 \times 10^3$) with the same film

Table 2. Characteristic Parameters of Polymers To Obtain χ-Parameters

polymers	R_g (Å)[a]	a (Å)[b]	L_0 (Å)	L_0/R_g
d-PB1	145	5.8	615	4.3
d-SBR	83	6.3[c]	370	4.5
d-PS	103	6.7	445	4.3
d-PMMA	98	6.5	450	4.6

[a] $R_g = \sqrt{N/6}\,a$. [b] Segment lengths (obtained from ref 50). [c] $a_{sbr}^2 = \phi_{ps}a_{ps}^2 + (1 - \phi_{ps})a_{pb}^2$ with volume fraction of d-PS (ϕ_{ps}).

thickness in CO_2.[23] However, the maxima of the higher M_w d-PS thin films at the ridge were much larger ($S_f = 0.25$ at $T = 36\ °C$ and $P = 8.2$ MPa and $S_f = 0.22$ for $T = 50\ °C$ and $P = 10.0$ MPa) than those shown in Figure 4. This is due to the fact that the anomalous swelling is scaled with the polymer radius of gyration (R_g).[18] In the case of higher M_w d-PS thin films, the value of L_0/R_g corresponds to 1.7 while that used in the present study is 4.3 (see Table 2). At further compression up to $P = 35.0$ MPa, S_f decreased to a constant value of approximately 0.1 for both temperature conditions. Chang et al.[9] measured the swelling of bulk PS by using a cathetometer in the pressure range up to 25 MPa at $T = 35$ and $50\ °C$ (Figure 4). To compare the swelling between the thin and bulk films, we assumed that the swelling of the thin films was uniaxial[19,20,33,34] while that of the bulk (S_b) was isotropic, i.e., $S_b = ((L - L_0)/L_0)^3$. From the figure we can see that the rate of swelling in the bulk is maximal near the critical pressure, and a plateau, with no minima, in the swelling at a value of about 0.1 occurs, which follows closely the increase in density of CO_2 with pressure, i.e., density-dependent enhancement in solvent quality. Consequently, except for the excess swelling region, the swelling behavior of d-PS thin films at $T = 36\ °C$ was in good agreement with that in the bulk. On the other hand, the swelling of the d-PS thin film at $T = 50\ °C$ exceeded 30% that of the bulk in the supercritical region. Similar deviation has been observed in PDMS thin film-CO_2 mixtures below P_c.[19] Some explanations concerning this deviation, such as the enhanced adsorption of CO_2 on the polymer thin film and polymer/CO_2 interface or a change in polymer chain conformation near a solid surface related to the bulk, were pointed out. Further studies are currently in progress.

(b) d-PB Thin Films. The similar swelling maxima were induced at the density fluctuation ridge in not only d-SBR ($S_f = 0.6$)[18] but also d-PS thin films. However, the maximal values were completely different between them even under the same scaled thickness ($L_0/R_g \sim 4.5$). To determine the effect of a random copolymer on the anomalous swelling, we examined d-PB thin films, which also have poor miscibility with CO_2 in the bulk. Note that the unswollen film thickness of 615 Å, which corresponds to $L_0/R_g = 4.3$ (see Table 2), was prepared to compare the swelling quantitatively. In Figure 5a S_f for d-PB1 thin film at $T = 36\ °C$ as a function of pressure is plotted. Compared with the swelling isotherm for d-SBR thin films,[18] the swelling behavior including the anomalous peak at the ridge is almost identical to that of d-SBR thin films. We can therefore conclude that the difference in the swelling at the ridge is not due to random copolymer composition but mainly the elasticity of the polymers.

Next, we focus on the R_g dependence of the swelling behavior for d-PB thin films. As we have already clarified, the anomalous swelling in d-PS thin films was
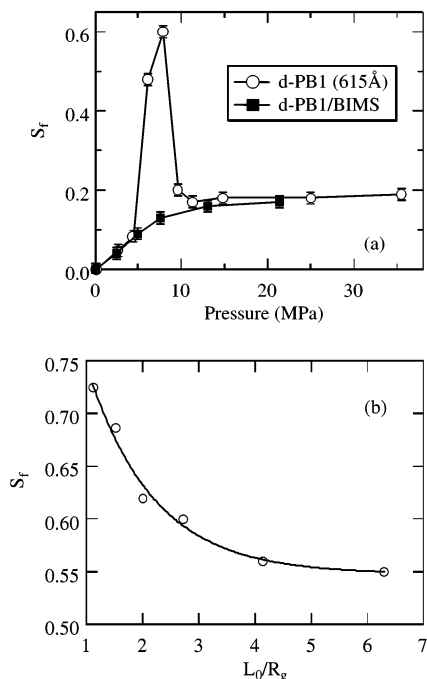
Figure 6. Time dependence of NR curves for d-PB–CO_2 mixture at $T = 36$ °C and $P = 8.2$ MPa.

Figure 5. (a) Pressure dependence of S_f for d-PB1 (open circles) and d-PB1/BIMS (filled squares) at $T = 36$ °C. (b) Excess swelling as a function of scaled thickness for d-PB. The solid line shows the best-fit result of the measured swelling with the exponential function (eq 4).

Figure 7. Linear dilation of d-PMMA as a function of pressure at $T = 36$ °C and 50 °C.

Table 3. Swelling Maxima in d-PB–CO_2 Mixtures at $T = 36$ °C and $P = 8.2$ MPa

polymer	L_0 (Å)	L_0/R_g (Å)	S_f
d-PB1	176	1.1	0.73
d-PB1	315	2.0	0.62
d-PB1	615	4.3	0.56
d-PB1	993	6.3	0.54
d-PB2	169	1.5	0.68
d-PB2	307	2.7	0.60

scaled by R_g and was a surface effect which occurs only within ~$10R_g$ thickness of the d-PS/CO_2 interface.[18] To explore whether the scaling behavior is a universal phenomena in thin films, we measured the R_g dependence of the swelling for the d-PB thin films. In Figure 5b we plot S_f for the d-PB thin films with varying thickness from 169 to 993 Å using two different M_w of d-PB at $T = 36$ °C and $P = 8.2$ MPa. The details are summarized in Table 3. From the figure, it is clear that as the scaled film thickness is increased, the S_f values at the ridge decrease. The S_f value reached 0.73 at $L_0/R_g = 1.1$. Especially, the S_f values drastically changed when the thickness was less than $3R_g$ and was in agreement with the exponential function shown by the solid line, i.e.,

$$S_f(T = 36 \text{ °C}, P = 8.2 \text{ MPa}) = 0.55 + 0.46 \exp[-0.85 L_0/R_g] \quad (4)$$

Similar exponential behavior of linear dilation was observed in d-PS thin films in CO_2.[18] However, two major differences can be pointed out: (i) the constant in the exponential function for d-PB is much larger than that for d-PS (0.44), indicating that the S_f values for d-PB change more drastically as a function of L_0/R_g, and (ii) the markedly larger S_f value (~0.55) at $L_0/R_g \sim 7$ for d-PB while that of d-PS is close to the bulk value. In this case the bulk swelling was simulated by using

the bilayer of brominated poly(isobutylene-*co*-*p*-methylstyrene) (BIMS) and d-PB, in which a 1 mm thick disk of BIMS was directly pressed onto the d-PB layer. The BIMS layer was not deuterated and served as a "cap" for the bottom d-PB film. If the penetration of density fluctuations is accessible down to the d-PB film, it is expected that a similar swelling peak at the ridge in the bilayer systems would be observed. As shown in Figure 5a, however, the NR measurements showed approximately an 8% swelling with no maxima at the ridge, indicating that the anomalous swelling in d-PB thin films disappeared in the bulk. Consequently, the polymer chains of d-PB films hold the high-stretching configurations even up to larger film thickness in the presence of large density fluctuations in CO_2. This insensitivity to the film thickness for d-PB thin films is analogous to that for PMMA films, which showed that the anomalous swelling existed even to 3210 Å, which is equivalent to the thickness of more than $25R_g$.[20]

At this point, it is important to detail the kinetics of the swelling at the ridge. Figure 6 shows the time dependence of the NR curves for the d-PB1 thin film ($L_0 = 615$ Å) at $T = 36$ °C and $P = 8.2$ MPa. From the figure, a 0.5 h annealing procedure, which is enough to reach the equilibrium swelling state for the glassy polymers including the ridge condition as well as the d-PB polymers except for the ridge condition, was not sufficient for d-PB films at the ridge. It was found that 4.5 h annealing was required to obtain the equilibrium swelling at the ridge. The change of the frequency in NR curves from 0.5 to 4.5 h annealing corresponds to a 30 Å increase in thickness. It should be noted that the d-SBR films also showed similar slow dynamics at the ridge, irrespective of the chain composition, indicating that the slow dynamics is mainly due to the high viscosity of the rubbery polymers.

(c) d-PMMA Thin Films. Figure 7 shows the pressure dependence of linear dilation for d-PMMA thin

films at $T = 36$ and 50 °C. From the figure we can see the similar anomalous peaks at the ridge, which are intermediate values between d-PS and d-PB under the same temperature and pressure conditions. Sirard et al. observed the similar swelling maxima in hydrogenated PMMA–CO_2 mixtures,[20] suggesting that the anomaly in the swelling behavior is independent of the deuteration of the polymers. As they pointed out, the anomalous swelling does not occur in the swelling of bulk PMMA.[7,8] A further interesting point is the swelling behavior in the higher pressure range between $20 < P < 70$ MPa, which is far beyond their accessible pressure range; S_f increased with increasing pressure to 0.45 while those of the d-PS, d-PB, and d-SBR thin films collapsed to the constant S_f values of 0.1–0.2. This indicates that the solvent quality of CO_2 in d-PMMA is much better than those in the other polymers at high pressure where the effect of density fluctuations can be ignored.[18] It is well-known that the better miscibility between CO_2 and PMMA is due to the specific intermolecular interaction between the PMMA carbonyl oxygen and the carbon atom of CO_2.[35] Hence, it is obvious that when processed as thin films, the solubility of CO_2 near the critical point is significantly enhanced by large density fluctuations in CO_2. It should be added that the S_f values of d-PMMA films at high pressures tend to decrease with increasing temperature, since the solubility depends on the CO_2 density as seen in the bulk.[7,8]

Discussion

There are two types of density inhomogeneities in SCFs with different length scales:[2,36] (a) long-range density inhomogeneities, which are referred to as "indirect density inhomogeneities" because of their indirect dependence on the solute–solvent interaction, i.e., solvent–solvent density correlations present in the compressible region; (b) short-range density inhomogeneities, so-called "direct density inhomogeneities", which are arise from the direct solute–solvent correlation.[37,38] Although the short-range density inhomogeneities are also influenced by the proximity of the solvent's critical point, they do not show the criticality, as seen in the long-range density inhomogeneities. It is well-known that the long-range density fluctuations influence the rate of increase in solubility with respect to temperature and pressure while the short-range ones control the absolute solubility. In contrast, the present study clearly proved that the long-range density inhomogeneities directly control the absolute solubility of CO_2 in the polymer thin films as a function of the magnitude of density fluctuations in CO_2. In addition, the comparison between the linear dilation and density fluctuation isotherms leads to an important conclusion: the anomalous swelling, which corresponds to the regions of $4.5 < P < 11.3$ MPa at $T = 36$ °C and $4.5 < P < 14.7$ MPa at $T = 50$ °C (see Figure 4), is induced with the condition of $\langle(\Delta N)^2\rangle/\langle N\rangle \geq 1.6$ for all the polymer thin films used in this study. Note that $\langle(\Delta N)^2\rangle/\langle N\rangle$ of 1 corresponds to that for the ideal gas state.

Next, we shall discuss the interaction parameter between CO_2 and polymers. Supercritical gas–polymer systems present special problems in order to express their $P–V–T$ properties since the two components are quite dissimilar. Polymer solution theory, such as the Flory–Huggins model, does not consider the volume change on the mixing so that it may not be an accurate model for polymer–CO_2 mixtures.[39] The lattice models, such as the Sanchez–Lacombe (S–L) equation of state or the Panayiotou–Vera equation of state models, have been used successfully to describe the thermodynamics of bulk polymer–supercritical mixtures.[7,8,14–16] Indeed, Zhang et al.[8] clarified that the bulk PS swelling behavior at $T = 35$ °C and in the range between $0 < P < 11$ MPa (see Figure 4) could be modeled accurately using the S–L equation of state. This indicates, however, that the S–L equation of state cannot describe the anomalous swelling in thin films near the ridge because the single adjustable parameter for polymer–CO_2 interactions in the S–L equation of state is constant at a fixed temperature. As Garg et al. pointed out,[14] there are still uncertainties in these equations of state models even in the bulk polymer–CO_2 mixtures because of the relatively poor thermodynamic modeling of CO_2 compared to that of the polymers.

To describe the phase equilibria of binary mixtures, Shim and Johnston[12] and Chang et al.[9] calculated the fugacity of CO_2 in both the polymers and fluid phase given by Prausnitz et al.[40] Combined with the Flory theory,[41] they could successfully express the swelling behavior of silicon rubber, PS, and poly(ethylene terephthalate) (PET) in CO_2. As mentioned above, the Flory theory is not ideal in expressing the thermodynamics of the polymers; however, as expressed in eq 5, it could be more convenient to use the volume fraction of CO_2 for expressing the combined effect of temperature and pressure on the interaction parameter.

According to the Flory theory for the fluid–polymer systems, the relation between χ and volume fraction of the polymer in the mixture, ϕ_p, is expressed as follows:

$$\ln(\alpha) = (\mu_1 - \mu_0)/RT =$$
$$\ln(1 - \phi_p) + (1 - 1/x)\phi_p + \chi\phi_p^2 \quad (5)$$

where α is the activity of the CO_2 in the polymer that is related to the chemical potential, μ_1 is the chemical potential of the solvent in the solution, μ_0 is the chemical potential in the pure liquid, and x is the ratio of the molar volumes of the polymer to solvent. The activity of CO_2 can be approximately expressed as $\alpha = P_1/P_1^0$ assuming the absence of the strong polymer–CO_2 interactions. However, Fleming and Koros pointed out that the approximation of the activity was not valid near the critical point.[11] Therefore, we used the equation derived by Prausnitz et al.[40] to express the activity of CO_2

$$\alpha = \frac{\sigma P}{P^{sat}\sigma^{sat}\exp\left(\dfrac{v^p(P - P^{sat})}{RT}\right)} \quad (6)$$

where σ is the fugacity coefficient, P^{sat} is the hypothetical vapor pressure, σ^{sat} is the fugacity coefficient at the vapor pressure, and v^p (= 46 cm^3/mol) is the molar volume of CO_2 in the polymer phase.[11] The value of P^{sat} in the polymer phase at $T = 36$ °C was determined from the log-linear extrapolation of the vapor pressure curve of CO_2.[11] The fugacity coefficient of CO_2, which describes nonideality of the fluid phase, was obtained from the Peng–Robinson equation of state.[42] To compare the interaction parameters for all the polymers used, the solubility data in the pressure range of $4.5 < P < 35.0$ MPa were chosen since the glassy polymers were adopted as the rubber state in the pressure range based on interdiffusion experiments by using NR.[24]
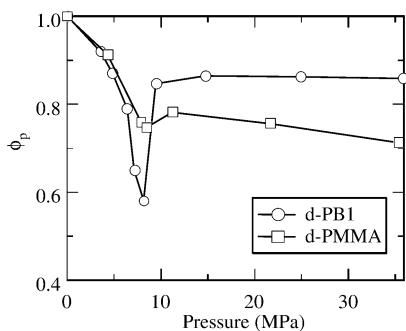
(8) Zhang, Y.; Gangwani, K. K.; Lemert, R. M. *J. Supercrit. Fluids* **1997**, *11*, 115.

(9) Chang, S. H.; Park, S. C.; Shim, J. J *J. Supercrit. Fluids* **1998**, *13*, 113.

(10) Goel, S. K.; Beckman, E. J. *Polymer* **1993**, *34*, 1410.

(11) Fleming, G. K.; Koros, W. J. *Macromolecules* **1986**, *19*, 2285.

(12) Shim, J. J.; Johnston, K. P. *AIChE J.* **1989**, *35*, 1097.

(13) Briscoe, B. J.; Zakaria, S. *J. Polym. Sci., Part B* **1991**, *29*, 989.

(14) Garg, A.; Gulari, E.; Manke, W. *Macromolecules* **1994**, *27*, 5643.

(15) Royer, J. R.; DeSimone, J. M.; Khan, S. A. *Macromolecules* **1999**, *32*, 8965.

(16) Kiszka, M. B.; Meilchen, M. A.; McHugh, M. A. *J. Appl. Polym. Sci.* **1988**, *36*, 583.

(17) Sanchez, I. C. *Physics of Polymer Surface and Interface*; Butterworth-Heinemann: Boston, 1992.

(18) Koga, T.; Seo, Y.-S.; Zhang, Y.; Shin, K.; Kusano, K.; Nishikawa, K.; Rafailovich, M. H.; Sokolov, J. C.; Chu, B.; Peiffer, D. G.; Satija, S. K. *Phys. Rev. Lett.* **2002**, *89*, 125506.

(19) Sirard, S. M.; Green, P. F.; Johnston, K. P. *J. Phys. Chem. B* **2001**, *105*, 766.

(20) Sirard, S. M.; Ziegler K. J.; Sanchez, I. C.; Green, P. F.; Johnston, K. P. *Macromolecules* **2002**, *35*, 1928. Although the anomalous swelling maxima have been reported, the relationship between the swelling maxima and the density fluctuation ridge was never mentioned in this work.

(21) McClain, J. B.; Londono, D.; Combes, J. R.; Romack, T. J.; Canelas, D. A.; Betts, D. E.; Wignall, G. D.; Samulski, E. T.; DeSimone, J. M. *J. Am. Chem. Soc.* **1996**, *118*, 917.

(22) Kendall, J. L.; Canelas, D. A.; Young, J. L.; DeSimone, J. M. *Chem. Rev.* **1999**, *99*, 543.

(23) Koga, T.; Shin, K.; Zhang, Y.; Seo, Y.-S.; Rafailovich, M. H.; Sokolov, J. C.; Chu, B.; Satija, S. K. *J. Phys. Soc. Jpn.*, *Suppl. A* **2001**, 347.

(24) Koga, T.; Seo, Y.-S.; Hu, X.; Kwanwoo, S.; Zhang, Y.; Rafailovich, M. H.; Sokolov, J. C.; Chu, B.; Satija, S. K. *Europhys. Lett.* **2002**, *60*, 559.

(25) Wang, W. V.; Kramer, E. J.; Sachse, W. H. *J. Polym. Sci., Polym. Phys. Ed.* **1982**, *20*, 1371.

(26) Condo, P. D.; Sanchez, I. C.; Panayiotou, C. G.; Johnston, K. P. *Macromolecules* **1992**, *25*, 6119.

(27) Condo, P. D.; Paul, D. R.; Johnston, K. P. *Macromolecules* **1994**, *27*, 365.

(28) Russell, T. P. *Mater. Sci. Rep.* **1990**, *5*, 171.

(29) Giddings, J. C.; Myers, M. N.; McLaren, L.; Keller, R. A. *Science* **1968**, *162*, 67.

(30) *Polymer Handbook*, 4th ed.; Brandrup, J., Immergut, E. H., Eds.; John Wiley & Sons: New York, 1999.

(31) Arora, K. A.; Lesser, A. J.; McCarthy, T. J. *Macromolecules* **1998**, *31*, 4614.

(32) Stafford, C. M.; Russell, T. P.; McCarthy, T. J. *Macromolecules* **1999**, *32*, 7610.

(33) Stamatialis, D. F.; Wessling, M.; Sanopoulou, M.; Strathmann, H.; Petropoulos, J. H. *J. Membr. Sci.* **1997**, *130*, 75.

(34) Sefcik, M. D. *J. Polym. Sci., Part B: Polym. Phys.* **1986**, *24*, 935.

(35) Kazarian, S. G.; Vincent, M. F.; Bright, F. V.; Liotta, C. L.; Eckert, C. A. *J. Am. Chem. Soc.* **1996**, *118*, 1729.

(36) Eckert, C. A.; Kuntson, B. L; Debenedetti, P. G. *Nature (London)* **1996**, *383*, 313.

(37) Chialvo, A. A.; Cummings, P. T. *AIChE J.* **1994**, *40*, 1558.

(38) Carlier, C.; Randolph, T. W. *AIChE J.* **1993**, *39*, 876.

(39) Maloney, D. P.; Prausnitz, J. M. *Ind. Eng. Chem. Process Des. Dev.* **1976**, *15*, 216.

(40) Prausnitz, J. M.; Lichtenthaler, R. N.; de Azevedo, E. G. *Molecular Thermodynamics of Fluid-Phase Equilibria;* Prentice-Hall: Englewood Cliffs, NJ, 1986; Chapter. 7.

(41) Flory, P. J. *Principle of Polymer Chemistry;* Cornell University Press: Ithaca, NY, 1969.

(42) Peng, D. Y.; Robinson, D. B. *Ind. Eng. Chem. Fundam.* **1976**, *15*, 59.

(43) Fleming, G. K.; Koros, W. J. *J. Polym. Sci., Part B: Polym. Phys.* **1987**, *25*, 2033.

(44) Karim, A.; Satija, S. K.; Douglas, J. F.; Ankner, J. F.; Fetters, L. J. *Phys. Rev. Lett.* **1994**, *73*, 3407.

(45) Milner, S. T.; Witten, T. A.; Cates, M. E. *Macromolecules* **1988**, *21*, 2610.

(46) Zhulina, E. B.; Borisov, O. V.; Pryamitsyn, V. A.; Birshtein, T. M. *Macromolecules* **1991**, *24*, 140.

(47) Lai, P. Y.; Binder, K. *J. Chem. Phys.* **1992**, *97*, 586.

(48) Grest, G. S.; Murat, M. *Macromolecules* **1993**, *26*, 3108.

(49) Koga, T.; et al. Manuscript in preparation.

(50) Pretel, E.; Rasmussen, A.; Rasmussen, P.; Holten-Andersen, J. *Macromolecules* **1997**, *30*, 2775.